Supplementary Information

Table of Contents

Supplemental Table 1. Phospholipids used to prepare liposomes in this study, and their physicochemical characteristics. All products were obtained from Avanti Polar Lipids.

Name	Catalog Number	Molecular Weight (g/mol)	Net Charge (0=Neutral; +1=Positive; -1=Negative)	Melting Temperature (ºC)
DSPC	850365C	790.145	0	55
DSPG	840465P	801.058	-1	55
Cholesterol	700100P	386.65	0	0
18:1 DOPG	840475P	797.026	-1	-18
18:1 DOPC	850375C	786.113	0	-17
14:0 DMPG	850345C	677.95	-1	23
14:0 DMPC	850345C	677.95	0	24
18:1 DGS-NTA(Ni)	790404	1057.003	0	0
18:1 DGS-NTA(Co)	791113	1057.24	0	0
DOPE	850725C	744.034	1	-16
DOPE-PEG(2000)-Cy5	880153C-1mg	3234.11	1	-16
POPG	840457C	770.989	-1	-2
DMG-PEG2000	880151	2509.2	0	Not provided
18:1 TAP (DOTAP)	890890	698.542	1	0

Supplemental Table 2. Liposome formulations reported as mole ratios.

Formulation	Lipids	Mole Ratio	Where Shown
1 (Standard)	DMPC – DMPG – cholesterol	9 – 1 – 2	Figures 1, 2, 3, 4, 5, 6, 7 & Supplemental Figures 1, 4
2 (Medium cholesterol)	DMPC – DMPG – cholesterol	9 – 1 – 6	Supplemental Figure 4
3 (High cholesterol)	DMPC – DMPG – cholesterol	9 – 1 – 10	Supplemental Figure 4
4 (Cationic)	DMPC – DOTAP – cholesterol	9 – 1 – 2	Supplemental Figure 2
5 (PEGylated)	DMPC – DMPG – cholesterol	13 – 2 – 4 – 1	Supplemental Figure 3
6 (Low Tm)	DOPC – DOPG – cholesterol	9 – 1 – 2	Supplemental Figure 5
7 (High Tm)	DSPC – DSPG – cholesterol	9 – 1 – 2	Supplemental Figure 5
8 (NTA-Ni functionalized)	DMPC – DMPG – cholesterol – DGS-NTA(Ni)	9 – 1 – 2 – 0.379	Figure 6 & Supplemental Figure 6
9 (NTA-Co functionalized)	DMPC – DMPG – cholesterol – DGS-NTA(Co)	9 – 1 – 2 – 0.379	Figure 6

Supplemental Table 3. Representative Dynamic Light Scattering of 50 nm extruded liposomes. Several Acquisitions of the Same Sample.

Item	Diameter (nm)	Normalized Intensity (Cnt/s)	Radius (nm)	%PD	Mw-R (kDa)	PD Index	Polydispersity (nm)
Acq 1	91.4	46655701	45.7	13	25769	1.31E-01	6
Acq 2	91.5	47009476	45.77	8.1	25859	8.07E-02	3.7
Acq 3	89.4	45015109	44.72	10.1	24497	1.01E-01	4.5
Acq 4	89.7	46480861	44.87	15.2	24686	1.52E-01	6.8
Acq 5	91.6	45287323	45.78	4.2	25867	4.17E-02	1.9
Acq 6	91.1	46959625	45.56	4.5	25586	4.49E-02	2
Acq 7	89.2	46312122	44.61	12.5	24355	1.25E-01	5.6
Acq 8	90	45467863	45.02	8.9	24881	8.92E-02	4
Acq 9	91.6	47301599	45.81	13.6	25906	1.36E-01	6.2
Acq 10	88.9	45506154	44.46	11	24164	1.10E-01	4.9

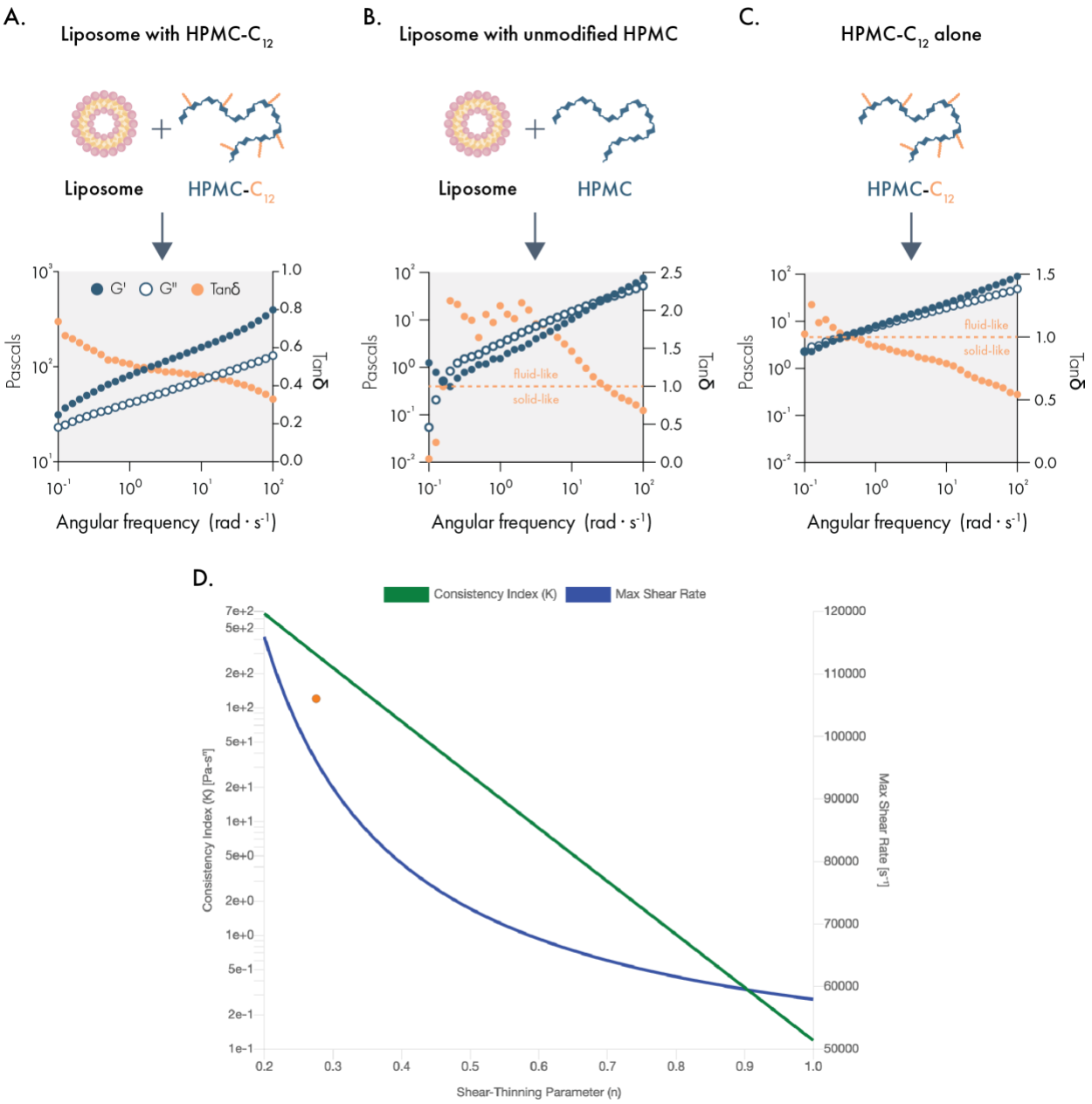

Supplemental Figure 1. Frequency sweep of liposomal hydrogels incorporating 2wt% hydroxypropylmethylcellulose (HPMC) with (**A**) and without (**B**) hydrophobic dodecyl (C_{12}) modification. Both formulations were prepared with 10wt% liposome content. **(C)** Rheological characterization of a 2wt% solution of HPMC- C_{12} without any liposomes. Elastic storage modulus (G') and viscous loss modulus (G'') across a wide range of frequencies on left y-axis. Tan(*delta*) is shown on the right y-axis, which can be used to determine whether the material exhibits solid or fluid properties. Dotted line indicates which Tan(*delta*) values indicate solid and liquid states. **D)** Ashby-style plot demonstrating the injectability of LNH (formulation 2PL10, orange dot) according the Lopez et al.[1] The consistency index *K* and shear-thinning parameter *n* were found using a power law fit. Formulations below the green line are considered injectable by humans through 27 G needles with lengths of 24.5 mm.

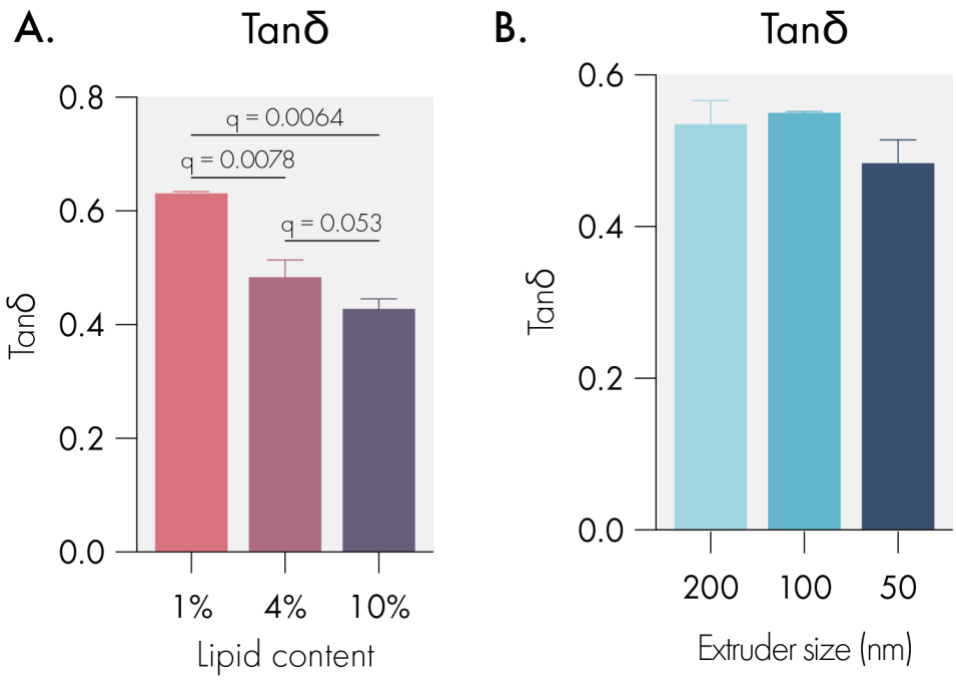

Supplemental Figure 2. Tan(delta) values at 10 rad/s, data represent mean and SEM of 2 replicate batches. (A) Tan(delta) varies with changes in overall lipid content of the hydrogels. (B) Tan(delta) is invariant with changing liposome size.

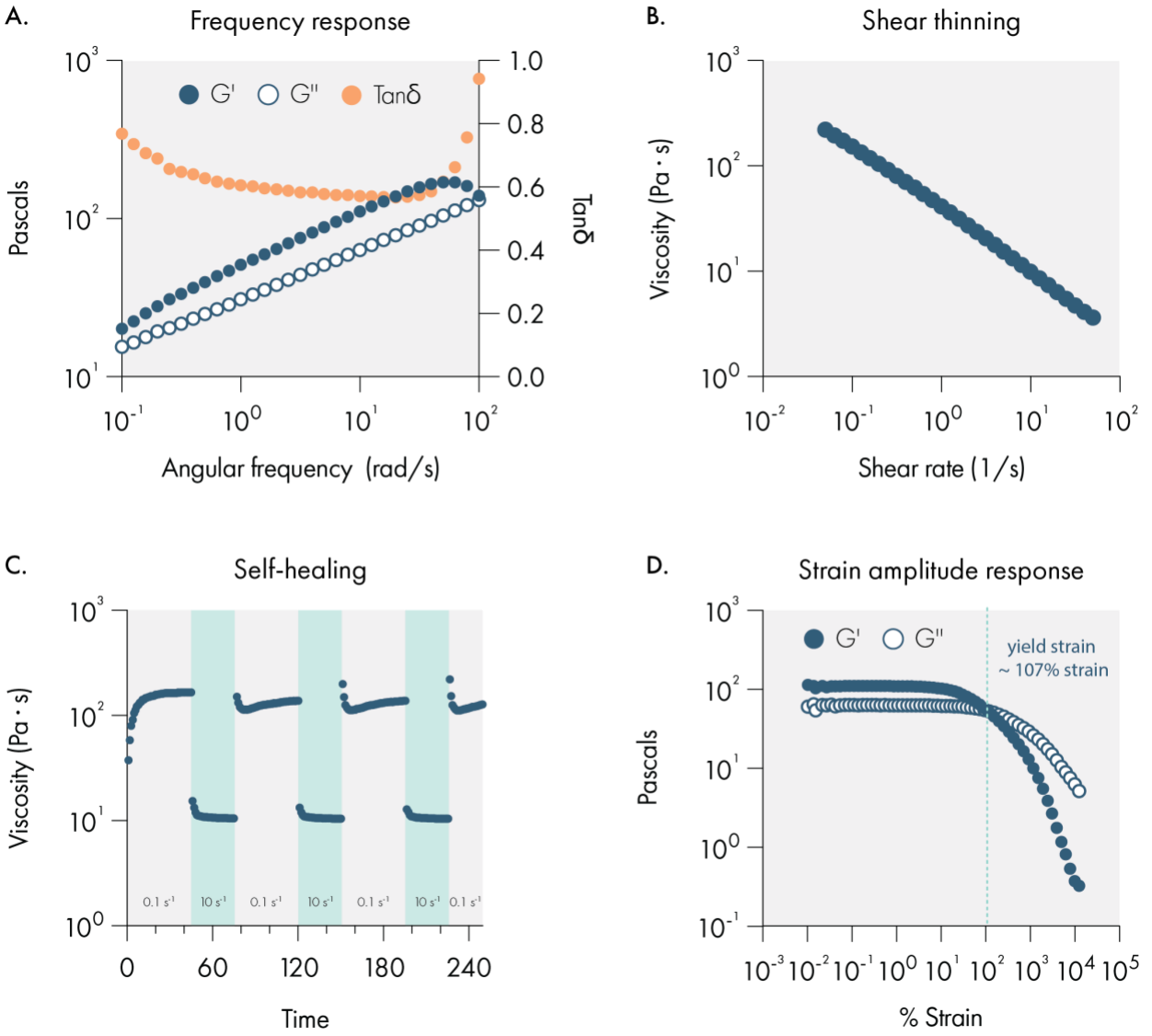

Supplemental Figure 3. Rheological properties of cationic liposomal hydrogels. (**A)** Frequency sweep demonstrating a gel-like response. (**B)** Flow sweep demonstrating the shear-thinning behavior. **(C)** Self-healing behavior demonstrated by cycling between a high (10 s^{-1}) and low (0.1 s^{-1}) shear rates with rapid recovery of the viscosity upon reduction of the shear rate. **(D)** Amplitude sweep assessing the linear viscoelastic regime and demonstrating the high % strain at yielding.

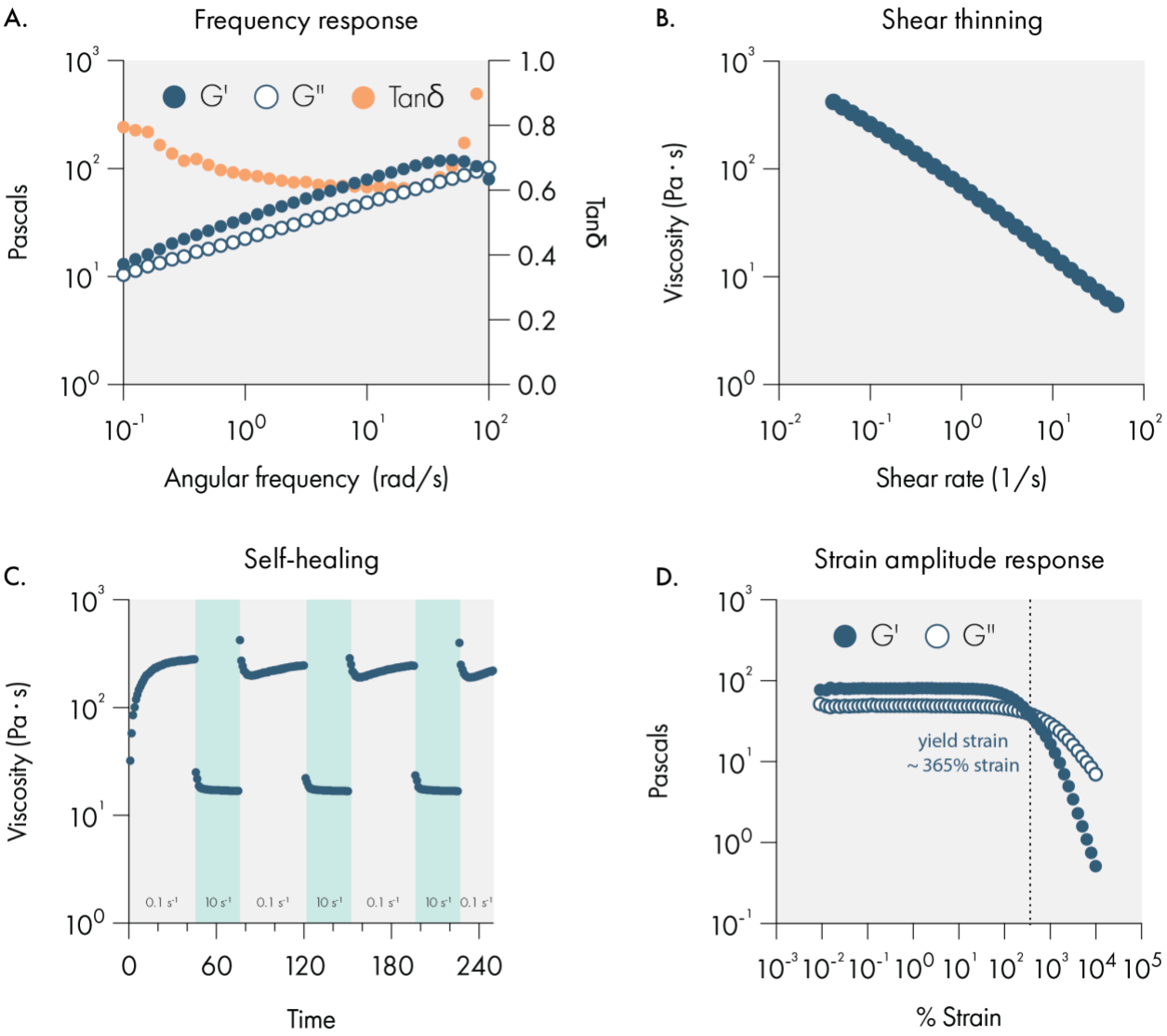

Supplemental Figure 4. Rheological properties of PEGylated liposomal hydrogels. **(A)** Frequency sweep demonstrating a gel-like response. **(B)** Flow sweep demonstrating the shear-thinning behavior. **(C)** Self-healing behavior demonstrated by cycling between a high (10 s-1) and low (0.1 s-1) shear rates with rapid recovery of the viscosity upon reduction of the shear rate. **(D)** Amplitude sweep assessing the linear viscoelastic regime and demonstrating the high % strain at yielding.

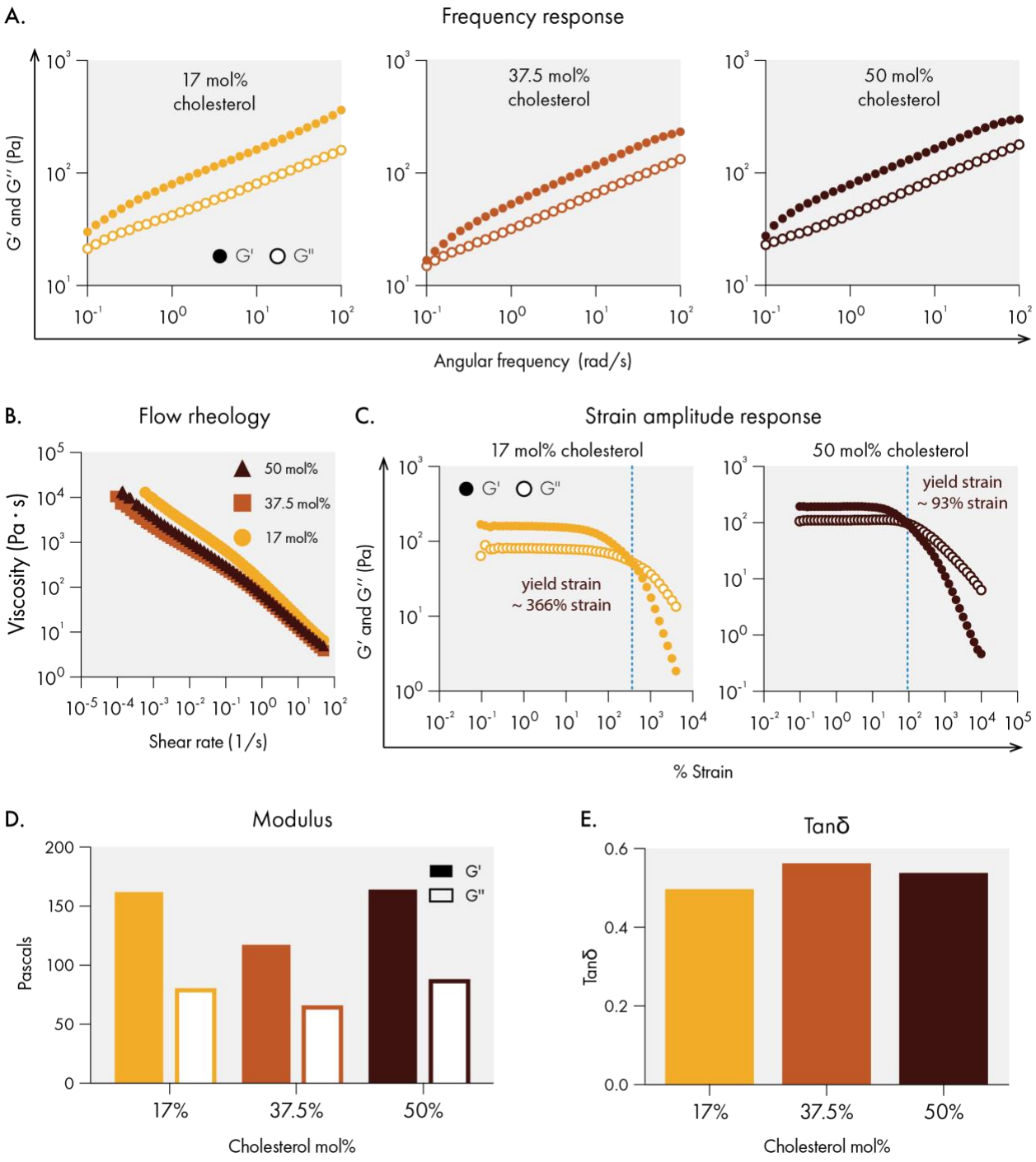

Supplemental Figure 5. Effect of cholesterol content on liposomal hydrogel rheological properties. **(A)** Frequency sweep demonstrating the relatively consistent gel-like response across several cholesterol mol% additions. **(B)** Flow sweep demonstrating the relatively consistent shear-thinning behavior across several cholesterol mol% additions. **(C)** Amplitude sweep assessing the linear viscoelastic regime and demonstrating the high % strain at yielding across several cholesterol mol % additions. **(D)** Elastic storage moduli (G') and viscous loss moduli (G'') at 1% strain and 10 rad/s of several cholesterol mol% additions. **E.** Tan(delta) at 1% strain and 10 rad/s of several cholesterol mol% additions.

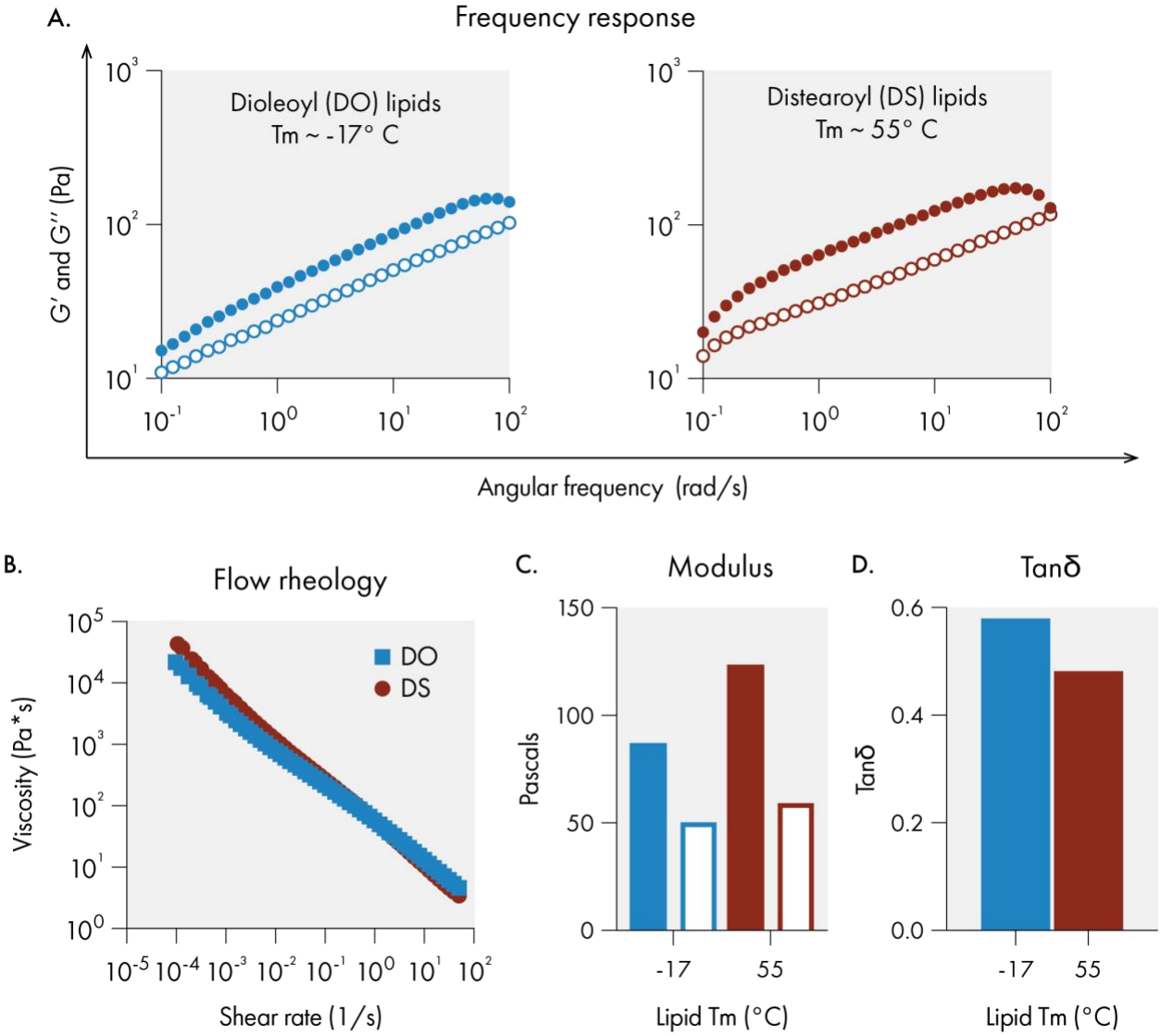

Supplemental Figure 6. Effect of varying the melting temperature (Tm) of the lipids comprising the liposomes in liposomal hydrogels. Dioleoyl lipids were incorporated for a low Tm, Distearoyl lipids were incorporated for a high Tm. **(A)** Frequency sweep demonstrating the relatively consistent gel-like response regardless of Tm. **(B)** Flow sweep demonstrating the relatively consistent shear-thinning behavior regardless of Tm. **(C)** Elastic storage moduli (G') and viscous loss moduli (G'') at 1% strain and 10 rad/s of liposomal hydrogels with varying Tm. **(D)** Tan(delta) at 1% strain and 10 rad/s of liposomal hydrogels with varying Tm. All measurements were conducted at room temperature.

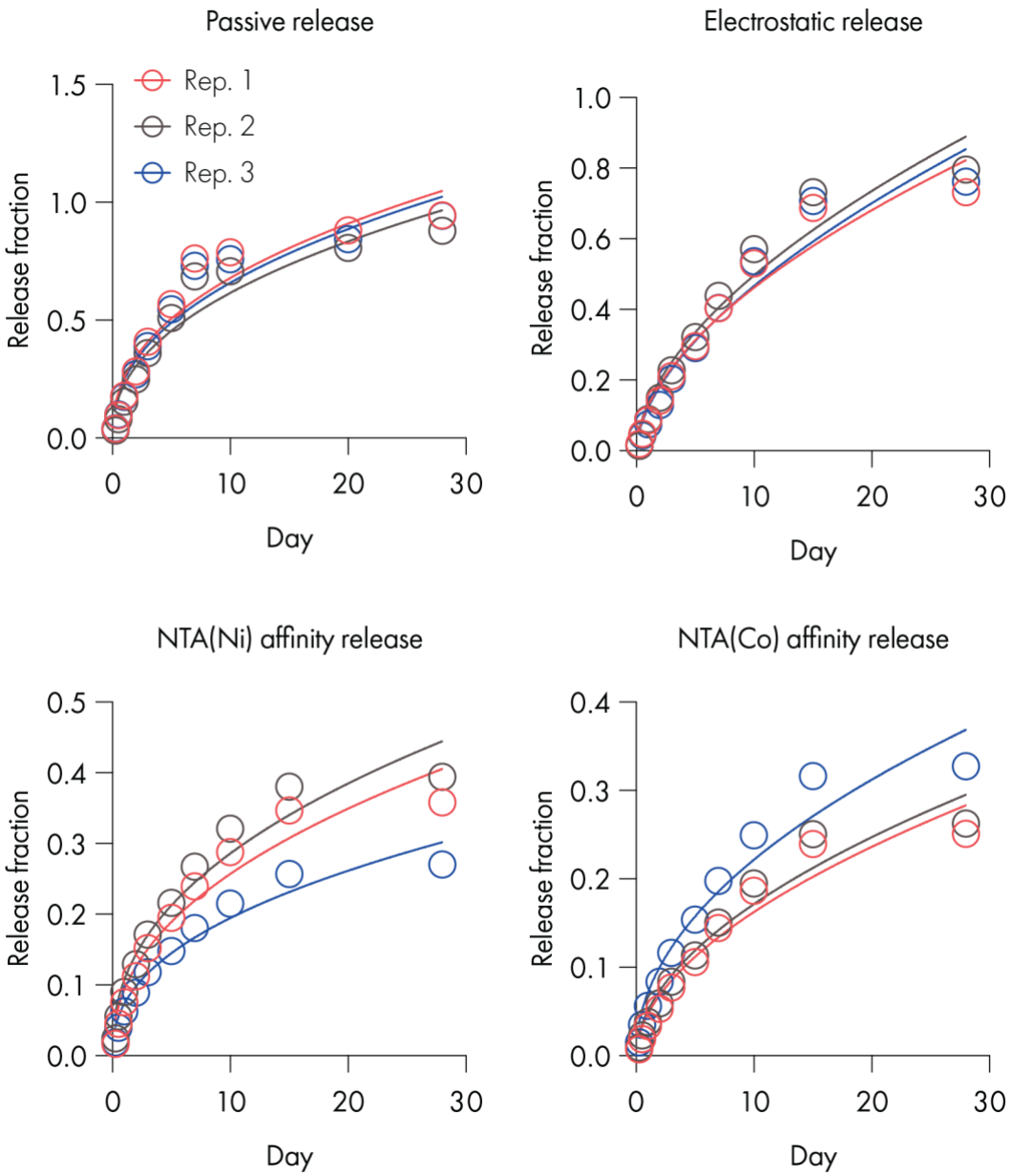

Supplemental Figure 7. Individual sample release curves of GFP from replicate hydrogels for several formulations of liposomal hydrogels that release cargo through different mechanisms with nonlinear Korsemeyer-Peppas fits.[2] Passive release is conducted with unmodified liposomes (Formulation 1 in Table 1) and GFP with no his tag. Electrostatic release is conducted with unmodified liposomes and GFP with a his tag. NTA(Ni) affinity release is conducted with hydrogels composed of 3 mol% NTA(Ni) modified liposomes (Formulation 8 in Table 1) and GFP with a his tag. NTA(Co) affinity release is conducted with hydrogels composed of 3 mol% NTA(Ni) modified liposomes (Formulation 9 in Table 1) and GFP with a his-tag.

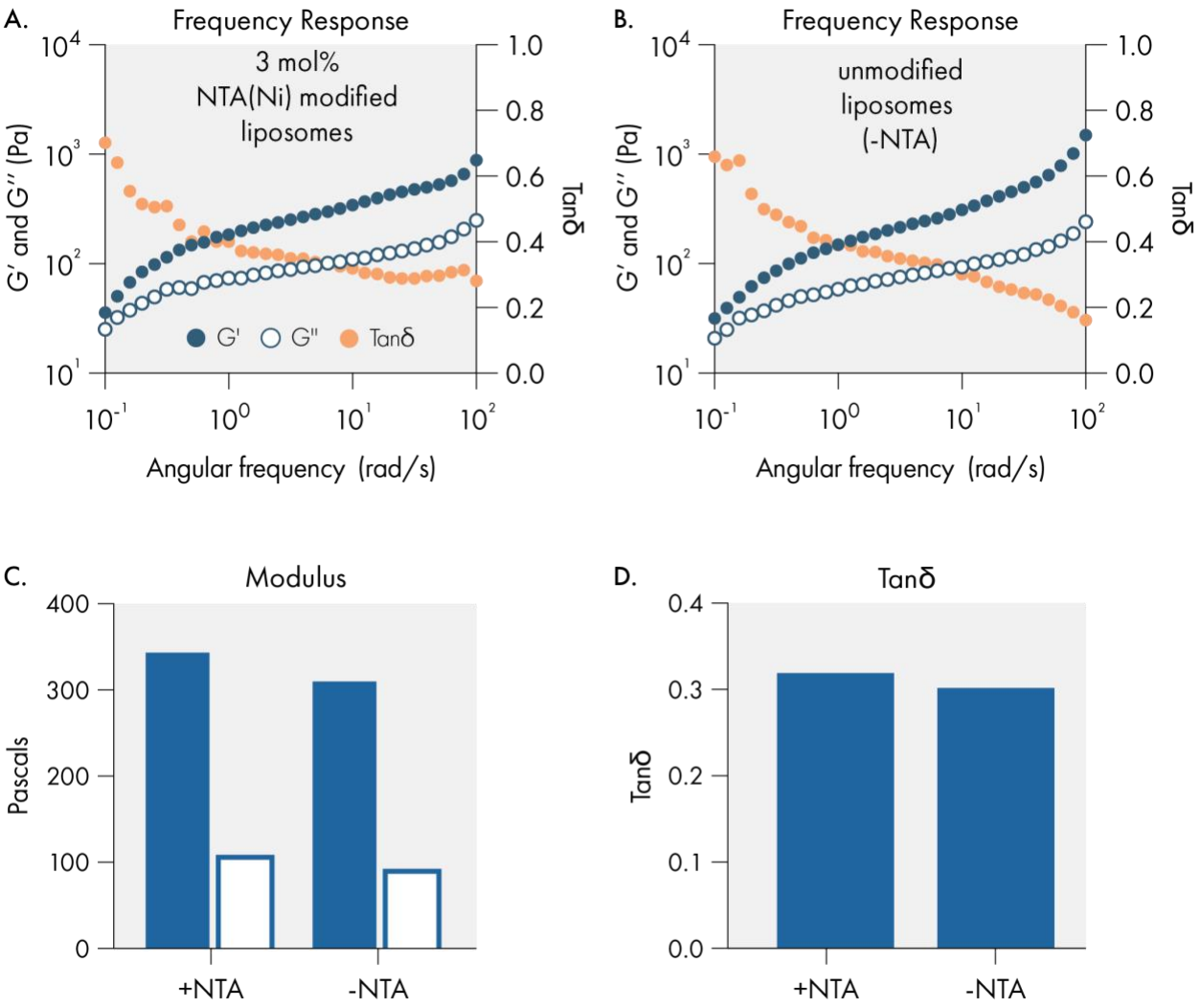

Supplemental Figure 8. Effect of 3 mol% NTA modified lipid incorporation on the rheological properties of liposomal hydrogels. No differences are observed. **(A)** Frequency sweep demonstrating the gel-like response. **(C)** Elastic storage moduli (G') and viscous loss moduli (G'') at 1% strain and 10 rad/s of both liposomal hydrogels. **(D)** Tan(delta) at 1% strain and 10 rad/s of both liposomal hydrogels. Both formulations were loaded with GFP to a final concentration 100 µg/mL. Rheological measurements were conducted using 8mm serrated parallel plates.

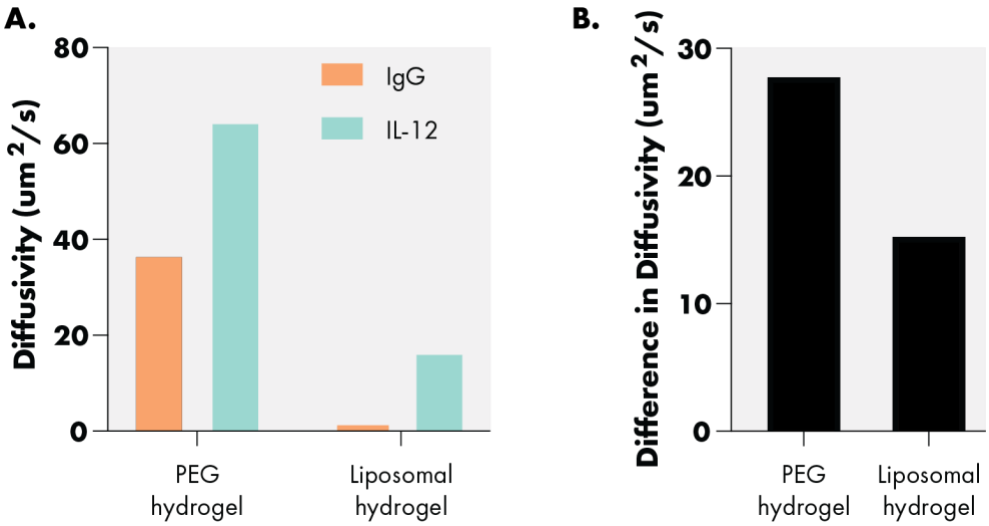

Supplementary Figure 9. Modeled diffusivity of IgG and IL-12 in hydrogels. **(A)** Predicted diffusivities of IgG antibodies and IL-12 cytokines in standard covalent PEG hydrogels and in liposomal hydrogels, assuming no matrix interaction with cargo (*e.g.*, passive release mechanisms).[3,4] **(B)** The predicted difference between the diffusivity of IL-12 and IgG antibody in each material. In the LNH IL-12 and IgG have closer diffusivity values.

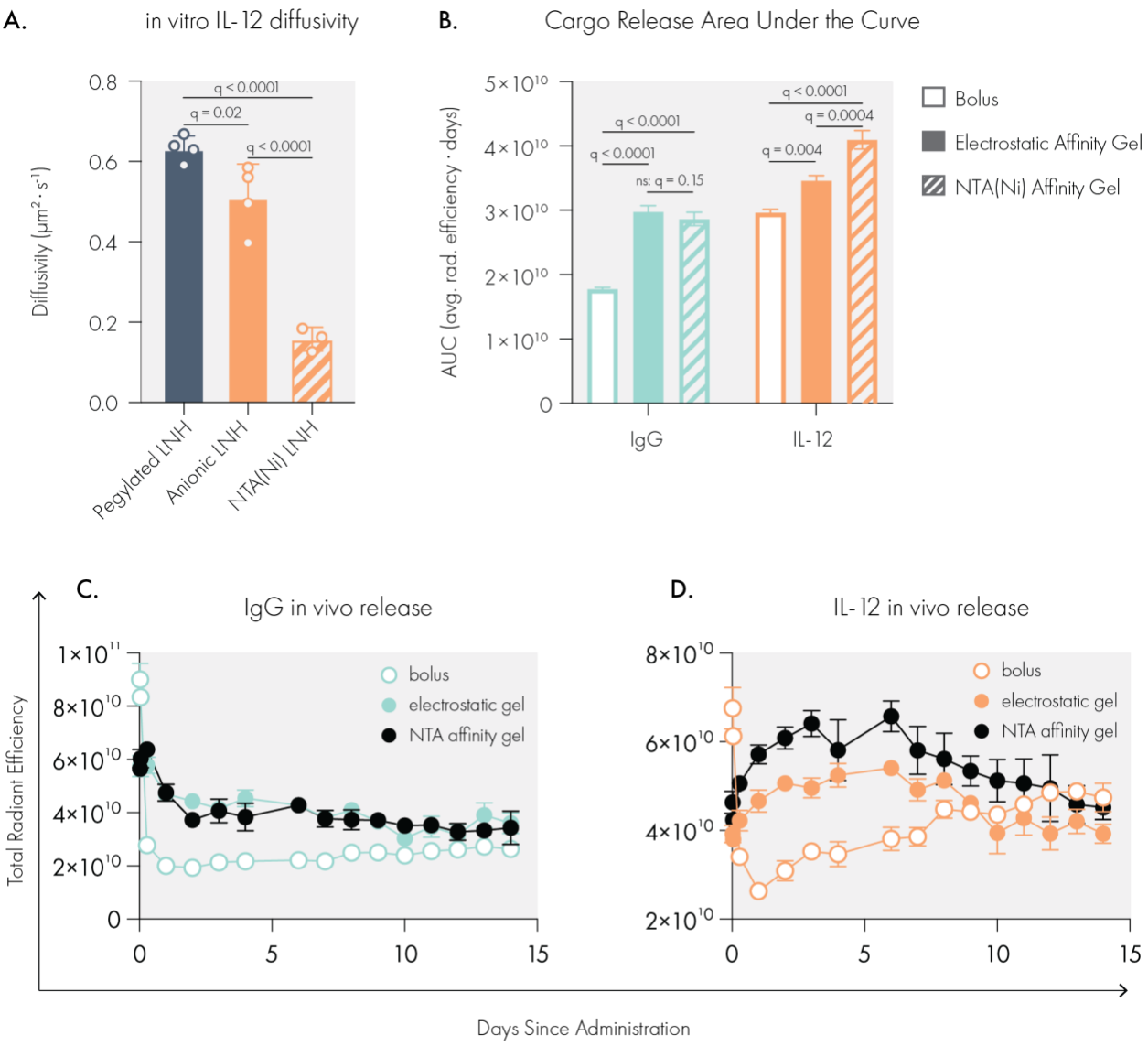

Supplemental Figure 10. IL-12 release *in vivo* is tuned by liposome surface chemistry. **(A)** *In vitro* preliminary analysis of IL-12 diffusion through liposomal hydrogels using FRAP. Mice were injected with liposomal hydrogels containing fluorescently labeled IgG and his-tagged IL-12. **(B)** Area under the curve was calculated for *in vivo* release data for IgG and IL-12 for each administration method. **(C)** IgG release data. **(D)** IL-12 release data.

References

1. Lopez Hernandez, H.; Souza, J. W.; Appel, E. A. (2021). A Quantitative Description for Designing the Extrudability of Shear-Thinning Physical Hydrogels. Macromol. Biosci. *21* (2), 2000295.
2. Wu, I. Y.; Bala, S.; Škalko-Basnet, N.; Di Cagno, M. P. (2019). Interpreting non-linear drug diffusion data: Utilizing Korsmeyer-Peppas model to study drug release from liposomes. Eur. J. of Pharm. Sci. *138*, 105026.
3. Axpe, E.; Chan, D.; Offeddu, G. S.; Chang, Y.; Merida, D.; Hernandez, H. L.; Appel, E. A. (2019). A multiscale model for solute diffusion in hydrogels. Macromolecules *52* (18), 6889.
4. Offeddu, G.; Axpe, E.; Harley, B.; Oyen, M. (2018). Relationship between permeability and diffusivity in polyethylene glycol hydrogels. AIP Adv. *8* (10), 105006.